Eur. Phys. J. B **54**, 189–200 (2006)
DOI: 10.1140/epjb/e2006-00445-9

THE EUROPEAN PHYSICAL JOURNAL B

Rashba billiards

A. Csordás[1], J. Cserti[2,a], A. Pályi[2], and U. Zülicke[3]

[1] Research Group for Statistical Physics of the Hungarian Academy of Sciences, Pázmány P. Sétány 1/A, 1117 Budapest, Hungary
[2] Department of Physics of Complex Systems, Eötvös University, 1117 Budapest, Pázmány Péter sétány 1/A, Hungary
[3] Institute of Fundamental Sciences and MacDiarmid Institute for Advanced Materials and Nanotechnology, Massey University, Private Bag 11 222, Palmerston North, New Zealand

Received 20 July 2006 / Received in final form 9 October 2006
Published online 22 December 2006 –

Abstract. We study the energy levels of non-interacting electrons confined to move in two-dimensional billiard regions and having a spin-dependent dynamics due to a finite Rashba spin splitting. The free space Green's function for such Rashba billiards is constructed analytically and used to find the area and perimeter contributions to the density of states, as well as the corresponding smooth counting function. We show that, in contrast to systems with spin-rotational invariance, Rashba billiards always possess a negative energy spectrum. A semi-classical analysis is presented to interpret the singular behavior of the density of states at certain negative energies for circular Rashba billiards. Our detailed analysis of the spin structure of circular Rashba billiards reveals a finite out-of-plane spin projection for electron eigenstates.

PACS. 73.21.La Quantum dots – 71.70.Ej Spin-orbit coupling, Zeeman and Stark splitting, Jahn-Teller effect – 05.45.Mt Quantum chaos; semiclassical methods – 03.65.Sq Semiclassical theories and applications

1 Introduction

Spin-dependent phenomena in semiconductor nanostructures have attracted great current interest [1,2]. Intriguing effects can arise in non-magnetic systems due to the presence of spin-orbit coupling. Structural inversion asymmetry in semiconductor heterostructures has been shown [3] to give rise to a spin splitting of the same type as was discussed in an early paper by Rashba [4]. Its tunability by external gate voltages [5–7] has motivated the theoretical design of a spin-controlled field-effect transistor [8]. Novel spin properties arise from the interplay between Rashba spin splitting and further confinement of two-dimensional electrons in quantum wires [9–12], rings [13,14], or dots [15–21]. Spin-orbit coupling has also been shown to affect the statistics of energy levels and eigenfunctions as well as current distributions [22,23]. The interplay between spin-orbit coupling and external magnetic fields was analyzed theoretically using random matrix theory [24].

In this work, we study *Rashba billiards*, i.e., non-interacting ballistic electrons moving in finite two-dimensional (2D) regions whose dynamics is affected by the Rashba spin-orbit coupling. In the one-band effective-mass approximation, the Hamiltonian with Rashba splitting in 2D is given by [25]

$$\hat{H} = \hat{H}_0 + \frac{\alpha}{\hbar}\hat{U}, \tag{1a}$$

$$\hat{H}_0 = \frac{p_x^2 + p_y^2}{2m^*} \tag{1b}$$

$$\hat{U} = \sigma_x p_y - \sigma_y p_x, \tag{1c}$$

where σ_x, σ_y are Pauli matrices. This Hamiltonian governs the electron dynamics inside the billiard with Dirichlet boundary conditions at the perimeter (see Ref. [18]). The Rashba spin-orbit coupling strength α can be conveniently measured in terms of a wave-number scale $k_{\rm so} = m^*\alpha/\hbar^2$, The spin-precession length defined as $\pi/k_{\rm so}$ can be tuned independently of the system size [5–7]. Furthermore, the tunability of the Rashba spin-orbit coupling strength is a convenient tool to induce changes of the billiard's energy spectrum without applying external magnetic fields.

One of our central quantity of interest is the density of states (DOS) $\varrho(E) = \sum_n \delta(E - E_n)$ and the counting function $N(E) = \sum_n \Theta(E - E_n)$ for Rashba billiards with energy levels E_n. Here $\delta(x)$ and $\Theta(x)$ are the Dirac delta function and the Heaviside function, respectively. The density of states and the counting function of normal billiards (without spin-orbit coupling, i.e., for $\alpha = 0$) have been extensively studied in the literature. They can be derived from the Green's function of the system. The smooth counting function $\bar{N}(E)$ is given by the so-called Weyl formula [26–28], which is an asymptotic series of the

[a] e-mail: cserti@complex.elte.hu

exact counting function $N(E)$, in terms of the energy E. A good introduction to this problem is given by Baltes and Hilf [27], and recently by Brack and Bhaduri [28], and many applications can be found in references [29–34].

We have derived the first two leading terms in the Weyl formula of the smooth counting function $\bar{N}(E)$ for arbitrary shapes of Rashba billiards. Our approach is based on the image method of Berry and Mondragon [35] developed for neutrino billiards, which have two-component wave functions and in this respect are rather similar to the Rashba billiards discussed here. We will show that the first term of $\bar{N}(E)$ is proportional to the area of the billiard, while the second one is proportional to the length of the perimeter of the billiard. Moreover, we find that the density of states is singular at the bottom of the spectrum. This singular behavior occurs independently of the billiard's shape and is most striking if the Rashba parameter is large.

The circular Rashba billiards is the simplest of confined systems that can be treated analytically [36–38]. Following the approach outlined above, we also calculate the smooth counting function $\bar{N}(E)$ for circular Rashba billiards, and besides its first two leading terms (which coincide with the results derived for arbitrary shapes of Rashba billiards) we give higher-order correction terms. Our analytical result for $\bar{N}(E)$ and that obtained from the numerically calculated exact energy levels are in perfect agreement.

In the absence of any lateral confinement, the energy dispersion for the Rashba Hamiltonian (1) splits into two branches [25]:

$$E(k_x, k_y) = \frac{\hbar^2}{2m^*}\left[(|\mathbf{k}| \pm k_{\mathrm{so}})^2 - k_{\mathrm{so}}^2\right], \qquad (2)$$

where $\mathbf{k} = (k_x, k_y)$. The spin splitting is a consequence of broken spin-rotational invariance. The spin of energy eigenstates, which are labeled by a 2D vector $\mathbf{k}$, is polarized perpendicularly to $\mathbf{k}$ [25]. Hence, no common spin quantization axis for single-electron states can be defined in the presence of spin-orbit coupling. As can be seen, in the range $0 < k < 2k_{\mathrm{so}}$, one branch has *negative energies* bounded from below by $-\Delta_{\mathrm{so}} \equiv -\hbar^2 k_{\mathrm{so}}^2/(2m^*)$.

Similarly, a laterally confined 2D system in the presence of Rashba type spin-orbit interactions has also a negative energy spectrum. In this paper, we present interesting features of the energy spectrum for circular Rashba billiards, focusing especially on its negative energy eigenvalues. We have found that for a circular shape, the density of states has additional singularities at negative energies. We obtain analytic results for their positions. Their corresponding eigenspinors have a finite spin projection in the direction perpendicular to the billiard plane, which is the direct result of imposing hard-wall boundary conditions.

Results presented in this article extend work reported in reference [39]. Its organisation is as follows. The properties of arbitrarily shaped Rashba billiards are discussed in Section 2. We present an algebraic expression for the free-space Green's function in the presence of Rashba spin-orbit coupling in Section 2.1. Subsequently, in Section 2.2, the first two leading terms of the Weyl formula are derived. Using the eigenstates presented in Section 2.3 in the absence of lateral confinement, we derive an alternative expression for the free-space Green's function in polar coordinates in Section 2.4. The circular Rashba billiards are discussed in Section 3. An analytical formula for the Green's function is derived in Section 3.1 for this case, while the derivation of the smooth counting function is presented in Section 3.2, including its comparison with the numerically calculated result. For negative energies the counting function is calculated in Section 3.3, while the spin structures is discussed in Section 3.4. Finally, our results are summarized and conclusions given in Section 4.

2 Arbitrary shapes of Rashba billiards

In this section we derive the smooth part of the density of states and the smooth part of the counting function, i.e., the two leading terms in the Weyl formula [26–28] for arbitrary shapes of Rashba billiards. These smooth functions are obtained by averaging the exact DOS and counting function over a small energy range around an energy E.

The exact density of states $\varrho(E)$ expressed in terms of the retarded Green's function (see e.g., [28]) is given by

$$\varrho(E) = -\frac{1}{\pi}\lim_{\eta\to 0^+} \mathrm{Im}\,\mathrm{Tr}\, G(E + i\eta, \mathbf{r}, \mathbf{r}'), \qquad (3)$$

where the trace means the limit $\mathbf{r} \to \mathbf{r}'$, integration of $\mathbf{r}$ over the area of the billiard, and the trace in spin space. The exact Green's function $G(z, \mathbf{r}, \mathbf{r}')$ is the position representation of the Green operator $\hat{G}(z) = (z - \hat{H})^{-1}$, which in addition, satisfies the boundary conditions. Then, the exact counting function is defined by $N(E) = \int_{-\infty}^{E} \varrho(E')dE'$.

Usually, the exact Green's function satisfying the boundary conditions is not known. However, one can always write the exact Green's function as a sum of the so-called free-space Green's function and a correction with which the exact Green's function satisfies the boundary conditions. The free-space Green's function $G_\infty(E, \mathbf{r}, \mathbf{r}')$ is the Green's function of the infinite system and does not satisfy the boundary conditions at the boundary of the billiards. In this paper, we calculate the free-space Green's function $G_\infty(E, \mathbf{r}, \mathbf{r}')$ for the Rashba Hamiltonian (1), and in case of circular Rashba billiards, the exact Green's function which satisfies the Dirichlet boundary conditions at the boundary of the billiards.

The first term in the Weyl formula, called area term, can be obtained by replacing the exact Green's function with the free-space Green's function $G_\infty(E, \mathbf{r}, \mathbf{r}')$ in equation (3). It is always proportional to the area of the billiard. Higher-order terms in the Weyl formula are the corrections to the area term taking into account the exact Green's function. The smooth part of the first correction term is called perimeter term because it is proportional to the length of the perimeter of the billiard.

2.1 Free-space Green's function for Rashba billiards

All our subsequent calculations are crucially based on the knowledge of the free-space Green's function $G_\infty(E,\mathbf{r},\mathbf{r}')$ for Rashba billiards. In this subsection, we present its derivation.

At a given energy E, two propagating modes exist whose wave vectors can be found from the dispersion relation (2):

$$|\mathbf{k}| = k_\pm = |k \mp k_{\rm so}|, \quad \text{where} \quad k = \sqrt{\frac{2m^*E}{\hbar^2} + k_{\rm so}^2}. \quad (4)$$

Using the identities for the Pauli matrices one can easily show that $\hat{U}^2 = p_x^2 + p_y^2$ and the Rashba Hamiltonian can be written as

$$\hat{H} = \frac{\hat{U}^2}{2m^*} + \frac{\alpha}{\hbar}\hat{U}.$$

The free-space Green operator $\hat{G}_\infty(E) = (E - \hat{H})^{-1}$ corresponding to the Rashba Hamiltonian reads then

$$\hat{G}_\infty(E) = \frac{2m^*}{\hbar^2}\left[\tilde{k}^2(E) - \left(\frac{\hat{U}}{\hbar} + k_{\rm so}\right)^2\right]^{-1}, \quad (5)$$

where $\tilde{k} = \sqrt{2m^*E/\hbar^2 + k_{\rm so}^2}$. Here E can be a complex number. Using the operator identity

$$\left(\lambda^2 - \hat{A}^2\right)^{-1} = \frac{1}{2\lambda}\left[\left(\lambda + \hat{A}\right)^{-1} + \left(\lambda - \hat{A}\right)^{-1}\right], \quad (6)$$

where λ is a scalar and $\hat{A}$ is an operator, one can decompose $\hat{G}_\infty(E)$ as

$$\hat{G}_\infty(E) = \frac{m^*}{\tilde{k}\hbar^2}\left[\left(\tilde{k}_- + \frac{\hat{U}}{\hbar}\right)^{-1} + \left(\tilde{k}_+ - \frac{\hat{U}}{\hbar}\right)^{-1}\right], \quad (7)$$

where $\tilde{k}_\pm = \tilde{k} \mp k_{\rm so}$. Now using the operator identity $\left(\lambda \pm \hat{A}\right)^{-1} = \left(\lambda \mp \hat{A}\right)\left(\lambda^2 - \hat{A}^2\right)^{-1}$, one finds

$$\hat{G}_\infty(E) = \frac{m^*}{\hbar^2}\frac{1}{\tilde{k}}\left[\left(\tilde{k}_- - \frac{\hat{U}}{\hbar}\right)\left(\tilde{k}_-^2 - \frac{\mathbf{p}^2}{\hbar^2}\right)^{-1} + \left(\tilde{k}_+ + \frac{\hat{U}}{\hbar}\right)\left(\tilde{k}_+^2 - \frac{\mathbf{p}^2}{\hbar^2}\right)^{-1}\right]. \quad (8)$$

The retarded Green's function in position representation is given by

$$G_\infty(E,\mathbf{r},\mathbf{r}') = \langle\mathbf{r}|\hat{G}_\infty(E + i\eta)|\mathbf{r}'\rangle, \quad (9)$$

where E is a real number and $\eta \to 0^+$. The two terms in equation (8) in position representation involve two functions:

$$\langle\mathbf{r}|\left(\tilde{k}_\pm^2 - \frac{\mathbf{p}^2}{\hbar^2}\right)^{-1}|\mathbf{r}'\rangle. \quad (10)$$

After a simple limiting procedure one can show that

$$\tilde{k}_+^2(E + i\eta) = k_+^2(E) + \mathrm{sgn}(E)\, i\eta, \quad (11a)$$

$$\tilde{k}_-^2(E + i\eta) = k_-^2(E) + i\eta, \quad (11b)$$

where $k_\pm$ are given by equation (4). The two functions in (10) can be evaluated by the following identities (see e.g., [28]):

$$\langle\mathbf{r}|\left(k^2 - \frac{\hat{\mathbf{p}}^2}{\hbar^2} \pm i\eta\right)^{-1}|\mathbf{r}'\rangle = \begin{cases} -\frac{i}{4}H_0^{(1)}(k|\mathbf{r} - \mathbf{r}'|), \\ \frac{i}{4}H_0^{(2)}(k|\mathbf{r} - \mathbf{r}'|), \end{cases} \quad (12)$$

where $H_0^{(1,2)}(x)$ are the Hankel functions of zero order, and $k > 0$.

Finally, using equations (8–12) we can easily find

$$G_\infty(E,\mathbf{r},\mathbf{r}') = \frac{-i}{4}\frac{m^*}{\hbar^2}\frac{1}{k}\begin{cases} \Big[\left(k_- - \frac{\hat{U}}{\hbar}\right)H_0^{(1)}(k_-|\mathbf{r} - \mathbf{r}'|) \\ + \left(k_+ + \frac{\hat{U}}{\hbar}\right)H_0^{(1)}(k_+|\mathbf{r} - \mathbf{r}'|)\Big], \\ \quad \text{for } E > 0, \\ \Big[\left(k_- - \frac{\hat{U}}{\hbar}\right)H_0^{(1)}(k_-|\mathbf{r} - \mathbf{r}'|) \\ - \left(-k_+ + \frac{\hat{U}}{\hbar}\right)H_0^{(2)}(k_+|\mathbf{r} - \mathbf{r}'|)\Big], \\ \quad \text{for } E < 0. \end{cases} \quad (13)$$

We note that, for negative energies E, the retarded Green's function contains incoming circular waves besides outgoing waves.

2.2 Area and perimeter terms of the density of states

First, consider the area term of the Weyl formula. Now, in equation (3) we replace the exact Green's function $G(E,\mathbf{r},\mathbf{r}')$ by the free-space Green's function $G_\infty(E,\mathbf{r},\mathbf{r}')$ given by equation (13). The trace of the operator $\hat{U}$ is zero since $\hat{U}$ is an off-diagonal matrix in the spin space. Then, it is easy to see that the leading term in the DOS becomes

$$\varrho_{\rm area}(E) = \frac{\mathcal{A}}{2\pi}\frac{2m^*}{\hbar^2}\frac{1}{k}\begin{cases} k, & \text{for } E > 0, \\ k_{\rm so}, & \text{for } E < 0, \end{cases} \quad (14)$$

where $\mathcal{A}$ is the area of the Rashba billiard. Therefore, the integration of the DOS yields the counting function:

$$N_{\rm area}(E) = \frac{\mathcal{A}}{\pi}\frac{2m^*}{\hbar^2}\begin{cases} \frac{E}{2} + \Delta_{\rm so}, & \text{for } E > 0, \\ \sqrt{\Delta_{\rm so}}\sqrt{E + \Delta_{\rm so}}, & \text{for } -\Delta_{\rm so} < E < 0. \end{cases} \quad (15)$$

It follows directly from equation (15) that, for negative energies, the DOS shows a $1/\sqrt{E + \Delta_{\rm so}}$ singularity at the bottom of the spectrum $E \to -\Delta_{\rm so}$. The area term (15) can alternatively be derived from the classical phase-space integral in the underlying classical approach. However, the classical dynamics of electrons in Rashba billiards is

described by *two* Hamiltonians [40], which are reminiscent of the two dispersion branches (2). The constant-energy surfaces in phase space are different for the two Hamiltonians, yielding different contributions to the classical phase-space integral. This simple calculation also leads to equation (15).

For arbitrary shapes of Rashba billiards, we can also determine the perimeter term of the DOS and the counting function. This term can be derived from the generalization of the image method of reference [30] using only the free space Green's function. The actual calculation is very much similar to that applied by Berry and Mondragon [35] for neutrino billiards. The Dirichlet boundary conditions can be approximately satisfied by regarding the boundary as straight and using the approximate Green's function

$$G(\mathbf{r},\mathbf{r}') \approx G_\infty(\mathbf{r},\mathbf{r}') + G_i(\mathbf{r},\mathbf{r}'), \text{ where} \tag{16a}$$
$$G_i(\mathbf{r},\mathbf{r}') \equiv -G_\infty(\mathbf{r},\mathbf{r}_i), \tag{16b}$$

and $\mathbf{r}_i$ is the image of $\mathbf{r}'$ on the boundary outside the billiard. Obviously $G(\mathbf{r},\mathbf{r}')$ is still a solution of the Schrödinger equation in the variable $\mathbf{r}$. To calculate the trace in (3) of $G_i(\mathbf{r},\mathbf{r}')$ we define $\mathbf{r} = (n,s)$ and $\mathbf{r}' = (n, s+\sigma)$, where n and s are the coordinates of $\mathbf{r}$ perpendicular to and along the boundary. Of course $n < 0$ since $\mathbf{r}$ is inside the billiard and the limit $\mathbf{r} \to \mathbf{r}'$ in the trace corresponds to $\sigma \to 0$. Now, $|\mathbf{r} - \mathbf{r}_i| = \sqrt{(2n)^2 + \sigma^2}$ and the correction to the DOS, i.e., $\varrho_{\mathrm{perim}}(E)$ coming from $G_i(\mathbf{r},\mathbf{r}')$ can be written as

$$\begin{aligned}\varrho_{\mathrm{perim}}(E) &= -\frac{1}{\pi}\lim_{\eta\to 0^+} \mathrm{Im}\,\mathrm{Tr}\;\hat{G}_i(E+i\eta,\mathbf{r},\mathbf{r}') \\ &= -\frac{1}{2\pi}\frac{m^*}{\hbar^2}\frac{1}{k}\int_0^{\mathcal{L}} ds \int_{-\infty}^{0} dn \\ &\quad\times [k_- J_0(k_- 2n) + k_+ J_0(k_+ 2n)],\end{aligned} \tag{17}$$

where the factor 2 of the trace in the spin space has already been included. Using the integral $\int_0^\infty J_0(ax)dx = 1/a$ with $a > 0$ we obtain

$$\varrho_{\mathrm{perim}}(E) = -\frac{\mathcal{L}}{4\pi}\frac{2m^*}{\hbar^2}\frac{1}{k}, \tag{18}$$

valid for all energies $E > -\Delta_{\mathrm{so}}$. Here $\mathcal{L}$ is the length of the perimeter of the billiard. Finally, the integration of the DOS yields the counting function:

$$N_{\mathrm{perim}}(E) = -\frac{\mathcal{L}}{2\pi}\sqrt{\frac{2m^*}{\hbar^2}}\sqrt{E+\Delta_{\mathrm{so}}}, \tag{19}$$

valid also for all energies $E > -\Delta_{\mathrm{so}}$. The minus sign is a consequence of Dirichlet boundary conditions.

In summary, the first two terms in the Weyl formula for arbitrary shapes of Rashba billiards reads as $\bar{N}(E) = N_{\mathrm{area}}(E) + N_{\mathrm{perim}}(E)$. Note that for zero spin–orbit coupling, $\bar{N}(E)$ coincides with the previously derived result for 2D billiards [27–29,31,32] (apart from a factor 2 due to spin).

2.3 Eigenstates for infinite systems

In this section the eigenvalues and eigenstates of the free-particle Rashba Hamiltonian given by equation (1) are calculated in polar coordinates. These results will be used in Section 2.4 to rewrite the free-space Green's function (13) in a form which is suitable for calculations in case of circular Rashba billiards presented in Section 3.

The Hamiltonian (1) can be rewritten in polar coordinates $\mathbf{r} = (r,\varphi)$ and we have $\hat{H} = \hat{H}_0 + \frac{\alpha}{\hbar}\hat{U}$, where

$$\hat{H}_0 = -\frac{\hbar^2}{2m^*}\left(\frac{\partial^2}{\partial r^2} + \frac{1}{r}\frac{\partial}{\partial r} + \frac{1}{r^2}\frac{\partial^2}{\partial\varphi^2}\right), \tag{20a}$$

$$\frac{\hat{U}}{\hbar} = \begin{pmatrix} 0 & e^{-i\varphi}\left(\frac{\partial}{\partial r} - \frac{i}{r}\frac{\partial}{\partial\varphi}\right) \\ -e^{i\varphi}\left(\frac{\partial}{\partial r} + \frac{i}{r}\frac{\partial}{\partial\varphi}\right) & 0 \end{pmatrix}. \tag{20b}$$

Since the Hamiltonian $\hat{H}$ commutes with the total angular momentum operator $\hat{J}_z = -i\hbar\partial_\varphi + \frac{\hbar}{2}\sigma_z$, the stationary Schrödinger equation $\hat{H}|\chi\rangle = E|\chi\rangle$ can be solved using the following ansatz [18,19]

$$\langle\,\mathbf{r}\,|\chi_m\rangle = \begin{pmatrix} C_1 Z_m(kr)e^{im\varphi} \\ C_2 Z_{m+1}(kr)e^{i(m+1)\varphi}\end{pmatrix}, \tag{21}$$

where m is an integer, $k > 0$ and $Z_m(x)$ can be any of the Bessel functions $J_m(x)$, $Y_m(x)$, and $H_m^{(1,2)}(x)$. With the help of the well-known recursion relations of Bessel functions

$$Z_m'(x) \pm \frac{m}{x}Z_m(x) = \pm Z_{m\mp1}(x), \tag{22}$$

one can show that the constants C_1 and C_2 satisfy

$$\begin{pmatrix} k^2 & 2kk_{so} \\ 2kk_{so} & k^2\end{pmatrix}\begin{pmatrix} C_1 \\ C_2\end{pmatrix} = \frac{2m^*E}{\hbar^2}\begin{pmatrix} C_1 \\ C_2\end{pmatrix}. \tag{23}$$

Hence for a given k the two eigenenergies $E_\pm$ are

$$E_\pm(k) = \frac{\hbar^2}{2m^*}\left[(k \pm k_{\mathrm{so}})^2 - k_{\mathrm{so}}^2\right]. \tag{24}$$

Since the eigenvalues of the Schrödinger equation are independent of the chosen coordinate systems the above eigenenergies should be the same as those given in equation (2), which is indeed the case when $k = |\mathbf{k}|$. The corresponding two non-trivial solutions for $C_1^\pm$ and $C_2^\pm$ are given by

$$\begin{aligned} C_1^\pm/C_2^\pm &= \pm 1, \quad \text{for } E > 0, \\ C_1^\pm/C_2^\pm &= -1, \quad \text{for } -\Delta_{\mathrm{so}} < E < 0.\end{aligned} \tag{25}$$

For a given E the two positive solutions of equation (24) for k are $k_\pm$ given by equation (4).

$$G_\infty(E,\mathbf{r},\mathbf{r}') = -\frac{im^*}{4\hbar^2 k}\begin{cases}\begin{pmatrix} k_- H_-^1 + k_+ H_+^1 & -e^{-i\varphi}\left(\frac{\partial}{\partial r} - \frac{i}{r}\frac{\partial}{\partial\varphi}\right)(H_-^1 - H_+^1) \\ e^{i\varphi}\left(\frac{\partial}{\partial r} + \frac{i}{r}\frac{\partial}{\partial\varphi}\right)(H_-^1 - H_+^1) & k_- H_-^1 + k_+ H_+^1 \end{pmatrix}, & E>0, \\ \begin{pmatrix} k_- H_-^1 + k_+ H_+^2 & -e^{-i\varphi}\left(\frac{\partial}{\partial r} - \frac{i}{r}\frac{\partial}{\partial\varphi}\right)(H_-^1 + H_+^2) \\ e^{i\varphi}\left(\frac{\partial}{\partial r} + \frac{i}{r}\frac{\partial}{\partial\varphi}\right)(H_-^1 + H_+^1) & k_- H_-^1 + k_+ H_+^2 \end{pmatrix}, & -\Delta_{\rm so} < E < 0, \end{cases} \tag{28}$$

We are now in a position to construct different eigenstates using the Bessel and Hankel functions. The eigenspinors regular at the origin are

$$\langle\,\mathbf{r}|\chi_m^\pm\rangle = \begin{cases}\begin{pmatrix}\pm J_m(k_\pm r)\\ J_{m+1}(k_\pm r)e^{i\varphi}\end{pmatrix}e^{im\varphi},\ E>0,\\ \begin{pmatrix}-J_m(k_\pm r)\\ J_{m+1}(k_\pm r)e^{i\varphi}\end{pmatrix}e^{im\varphi},\ E<0.\end{cases} \tag{26}$$

To derive the free-space Green's function in polar coordinates we shall also use solutions which are singular at the origin:

$$\langle\,\mathbf{r}|h_m^\pm\rangle = \begin{pmatrix}\pm H_m^{(1)}(k_\pm r)\\ H_{m+1}^{(1)}(k_\pm r)e^{i\varphi}\end{pmatrix}e^{im\varphi},\quad E>0, \tag{27a}$$

$$\langle\,\mathbf{r}|h_m^+\rangle = \begin{pmatrix}-H_m^{(2)}(k_+ r)\\ H_{m+1}^{(2)}(k_+ r)e^{i\varphi}\end{pmatrix}e^{im\varphi},\quad E<0, \tag{27b}$$

$$\langle\,\mathbf{r}|h_m^-\rangle = \begin{pmatrix}-H_m^{(1)}(k_- r)\\ H_{m+1}^{(1)}(k_- r)e^{i\varphi}\end{pmatrix}e^{im\varphi},\quad E<0. \tag{27c}$$

2.4 Free-space Green's function in polar coordinates

Using (13) and (20b) the free-space retarded Green's function in the two energy ranges becomes

see equation (28) above

where we used the notations $H_\pm^{1,2} \equiv H_0^{(1,2)}(k_\pm|\mathbf{r}-\mathbf{r}'|)$. In the off-diagonal elements the differentiations with respect to r and φ can be carried out by introducing a new variable $\boldsymbol{\rho} = \mathbf{r} - \mathbf{r}'$. Then, for $E>0$ our simple algebraic method yields the same result that was derived by Walls et al. [42] using a different approach. However, they do not present any explicit form for $E<0$.

In our previous paper [39] we used another form for the free-space Green's function (although as a lack of space it was not published there) in order to determine exactly the Green's function for circular Rashba billiards. In this approach differentiations with respect to r and φ in the off-diagonal elements were performed using the addition theorem of the Bessel functions [43]

$$H_0^{(1,2)}(|\mathbf{r}-\mathbf{r}'|) = \sum_{m=-\infty}^{\infty} H_m^{(1,2)}(r)J_m(r')e^{im(\varphi-\varphi')},\quad r>r' \tag{29}$$

and the recursion relations (22). Then, for the free-space Green's function in polar coordinates for $r>r'$ we obtain a rather compact form in terms of the spinors defined in (26, 27):

$$G_\infty(\mathbf{r},\mathbf{r}') = c\sum_{m=-\infty}^{\infty}\Big[k_+\langle\mathbf{r}|h_m^+\rangle\langle\chi_m^+|\mathbf{r}'\rangle + k_-\langle\mathbf{r}|h_m^-\rangle\langle\chi_m^-|\mathbf{r}'\rangle\Big], \tag{30}$$

where $c = -im^*/(4\hbar^2 k)$. We shall use this form in Section 3.1.

3 Circular Rashba billiards

We now consider a circular Rashba billiard of radius R. The eigenstates of the system can be written as a linear combination of the regular eigenspinors given by equation (26) and the linear combination coefficients are chosen such that the eigenstates satisfy the Dirichlet boundary conditions. The straightforward calculation yields the following secular equation:

$$J_m(k_+R)J_{m+1}(k_-R) + \mathrm{sgn}(E)J_m(k_-R)J_{m+1}(k_+R) = 0, \tag{31}$$

where m is an integer. For each quantum number m the solutions of this equation for E give the energy levels of the circular Rashba billiards. The same secular equation was derived in references [36–38]. This equation is invariant under the change $m \to -m-1$ (Kramers degeneracy). Formal solutions of the secular equation having zero wave vectors k_+ or k_- are excluded since the corresponding wave functions vanish everywhere inside the billiard ($E=0$). Similarly, the formal solution at $E=-\Delta_{\rm so}$ should also be excluded.

Following the ideas of the systematic method of Berry and Howls [32], we have calculated the first few leading terms of the smooth counting function $\bar{N}(E)$. To do this we need the exact Green's function for circular Rashba billiards which is calculated in the following subsection.

3.1 Green's function for circular Rashba billiards

Boundary conditions for billiards requires that the Green's function should vanish at the boundary (i.e., if either $\mathbf{r}$ or $\mathbf{r}'$ is on the perimeter). The free-space Green's function (30) for a given energy usually does not vanish at the boundary of the billiard. To fulfill the billiard boundary conditions we look for the exact Green operator, as usual, in the form of $\hat{G} = \hat{G}_\infty + \hat{G}_H$, where the homogeneous

Green's function satisfies $\left(E-\hat{H}\right)\hat{G}_H=0$. The boundary conditions for $\hat{G}$ are

$$G(\mathbf{r},\mathbf{r}')=G_\infty(\mathbf{r},\mathbf{r}')+G_H(\mathbf{r},\mathbf{r}')=0,\quad \text{for}\quad |\mathbf{r}|=R, \tag{32}$$

where $\mathbf{r}'$ is inside the billiard. Since the homogeneous Green's function $\hat{G}_H$ satisfies the same Schrödinger equation as the regular solutions given by equation (26) one can construct $\hat{G}_H$ from these eigenstates as

$$\hat{G}_H=\sum_{m=-\infty}^{\infty}\Big[\,A_m\,|\chi_m^+\rangle\langle\chi_m^+|+B_m\,|\chi_m^-\rangle\langle\chi_m^+| +C_m\,|\chi_m^+\rangle\langle\chi_m^-|+D_m\,|\chi_m^-\rangle\langle\chi_m^-|\,\Big], \tag{33}$$

where the constants A_m, B_m, C_m, and D_m, in principle, can be determined from the boundary conditions (32). For arbitrary shapes of billiards it results in an infinite set of linear equations for the constants. Fortunately, in case of circular billiards the constants can be determined analytically. Indeed, substituting equations (30) and (33) into equation (32), and identifying the coefficients of the eigenspinors $\langle\chi_m^\pm|\mathbf{r}'\rangle$ one finds

$$A_m\,\langle\mathbf{r}|\chi_m^+\rangle+B_m\,\langle\mathbf{r}|\chi_m^-\rangle=-c\,k_+\,\langle\mathbf{r}|h_m^+\rangle, \tag{34a}$$

$$C_m\,\langle\mathbf{r}|\chi_m^+\rangle+D_m\,\langle\mathbf{r}|\chi_m^-\rangle=-c\,k_-\,\langle\mathbf{r}|h_m^-\rangle, \tag{34b}$$

where the eigenspinors are evaluated at $|\mathbf{r}|=R$. These equations, in fact, are four independent linear inhomogeneous equations for A_m, B_m, C_m, and D_m since each eigenspinor is a two component vector. The solutions can be easily obtained from the appropriate determinants formed from the coefficients of equation (34), and are given by

$$A_m=-\frac{c\,k_+}{F_m}\begin{cases}\begin{vmatrix} H_m^{(1)}(k_+R) & -J_m(k_-R)\\ H_{m+1}^{(1)}(k_+R) & J_{m+1}(k_-R)\end{vmatrix}, & E>0,\\[2ex] \begin{vmatrix} -H_m^{(2)}(k_+R) & -J_m(k_-R)\\ H_{m+1}^{(2)}(k_+R) & J_{m+1}(k_-R)\end{vmatrix}, & E<0,\end{cases} \tag{35a}$$

$$D_m=-\frac{c\,k_-}{F_m}\begin{cases}\begin{vmatrix} J_m(k_+R) & -H_m^{(1)}(k_-R)\\ J_{m+1}(k_+R) & H_{m+1}^{(1)}(k_-R)\end{vmatrix}, & E>0,\\[2ex] \begin{vmatrix} -J_m(k_+R) & -H_m^{(1)}(k_-R)\\ J_{m+1}(k_+R) & H_{m+1}^{(1)}(k_-R)\end{vmatrix}, & E<0,\end{cases} \tag{35b}$$

$$B_m=C_m=\frac{2ic}{\pi RF_m},\quad \text{where} \tag{35c}$$

$$F_m=J_m(k_+R)J_{m+1}(k_-R)+\mathrm{sgn}(E)J_m(k_-R)J_{m+1}(k_+R). \tag{35d}$$

In equation (35c) we used the Wronskian relations for the Bessel functions [43].

Finally, the analytical form of the exact retarded Green's function of circular Rashba billiards in polar coordinates is a sum of the free-space Green's function $G_\infty(\mathbf{r},\mathbf{r}')$ given by equations (28) or (30), and the homogeneous part $G_H(\mathbf{r},\mathbf{r}')=\langle\mathbf{r}|\hat{G}_H|\mathbf{r}'\rangle$, where the operator $\hat{G}_H$ is given by equation (33) together with equation (35).

The eigenenergies of any billiards can be obtained from the poles of the retarded Green's function $\hat{G}$. For circular Rashba billiards the poles of $\hat{G}$ are the poles of $\hat{G}_H$, i.e., the zeros of F_m. As can be seen it yields the same secular equation (31) derived independently, and thus it provides one check point for the Green's function $\hat{G}_H$.

3.2 The smooth part of the density of states

To calculate the DOS and the counting function for circular Rashba billiards we adopt the ideas of the systematic method of Berry and Howls [32]. The exact Green operator of the system is $\hat{G}=\hat{G}_\infty+\hat{G}_H$. The first term of the density of states (3) is the contribution from $\hat{G}_\infty$ in the trace of $\hat{G}$. The result is given in (14), while the leading term in the counting function $N(E)$ is given by (15).

The correction terms of the DOS can be obtained from the trace of $\hat{G}_H$ given by equation (33). This involves the limit $\mathbf{r}\to\mathbf{r}'$, the trace of the 2 by 2 matrix $G_H(\mathbf{r},\mathbf{r})$ (trace over spinor indices) and the integration over the area of the billiard. After a straightforward calculation we found

$$\mathrm{Tr}\,\hat{G}_H=2\pi\sum_{m=-\infty}^{\infty}\int_0^R rdr\Big[J_m^2(k_+r)(A_{m-1}+A_m) +J_m^2(k_-r)(D_{m-1}+D_m) +2J_m(k_+r)J_m(k_-r)\begin{cases}(B_{m-1}-B_m), & E>0\\ (B_{m-1}+B_m), & E<0\end{cases}\Big]. \tag{36}$$

In the series with terms A_{m-1} the summation index m has been shifted by one to have the same radial integral as that in the series for A_m, and the same trick was done for series containing B_{m-1}, C_{m-1} and D_{m-1}.

The radial integrals in (36) can be performed analytically [44]. To calculate the density of states one needs to evaluate $\mathrm{Tr}\,\hat{G}_H$ at complex energies $E+i\eta$. To this end we follow the approach originally applied by Stewartson and Waechter [31], and later for example Berry and Howls [32], and the Bessel functions of the first kind $J_m(z)$ and $H_0^{(1,2)}(z)$ are converted to the modified Bessel functions $I_m(z)$ and $K_m(z)$ by extending the energy E to the complex plane. This is the so-called heat-kernel method. However, in our case one has to be careful for negative energies. It turns out that the parameters x, x_+ and x_- depending on energy E (here E is real) and defined as

$$ix\equiv R\,k(E+i\eta), \tag{37a}$$

$$ix_+\equiv \mathrm{sgn}(E)R\,k_+(E+i\eta), \tag{37b}$$

$$ix_-\equiv R\,k_-(E+i\eta), \tag{37c}$$

are useful to convert the Bessel functions of the first kind to the modified Bessel functions using the identities

$$J_m(iz) = i^m I_m(z), \tag{38a}$$

$$H_m^{(1)}(iz) = \frac{2}{\pi}(-i)^{m+1}K_m(z),\ -\pi < \arg z \le \frac{\pi}{2}, \tag{38b}$$

$$H_m^{(2)}(-iz) = \frac{2}{\pi}i^{m+1}K_m(z),\ -\frac{\pi}{2} < \arg z \le \pi. \tag{38c}$$

After a tedious algebra the result of these transformations in equation (36) can be written as

$$\mathrm{Tr}\,\hat{G}_H(E+i\eta) = \frac{m^*R^2}{\hbar^2 x}\sum_{m=-\infty}^{\infty} f_m(E+i\eta), \quad \text{where}$$

$$f_m(E+i\eta) = \left[1+\frac{m^2}{x_+^2} - \left(\frac{I'_m(x_+)}{I_m(x_+)}\right)^2\right] x_+ I_m(x_+) \times K_m(x_+) + \left[1+\frac{m^2}{x_-^2} - \left(\frac{I'_m(x_-)}{I_m(x_-)}\right)^2\right] x_- I_m(x_-)K_m(x_-)$$

$$-\frac{P_m(x_+,x_-)}{2}\left[1+\frac{m^2}{x_+^2} - \left(\frac{I'_m(x_+)}{I_m(x_+)}\right)^2 + 1 + \frac{m^2}{x_-^2} - \left(\frac{I'_m(x_-)}{I_m(x_-)}\right)^2 - \frac{4}{x_+^2 - x_-^2}\left(x_+\frac{I'_m(x_+)}{I_m(x_+)} - x_-\frac{I'_m(x_-)}{I_m(x_-)}\right)\right], \tag{39a}$$

and

$$P_m(x_+,x_-) = \frac{1}{\dfrac{I'_m(x_+)}{I_m(x_+)} + \dfrac{I'_m(x_-)}{I_m(x_-)} - \dfrac{m}{x_+} - \dfrac{m}{x_-} + \dfrac{1}{\dfrac{I'_m(x_+)}{I_m(x_+)} + \dfrac{I'_m(x_-)}{I_m(x_-)} + \dfrac{m}{x_+} + \dfrac{m}{x_-}}}. \tag{39b}$$

Up to now the trace of G_H for circular Rashba billiards is exact. Note that the above mentioned transformations result in the same form of $\mathrm{Tr}\,\hat{G}_H(E+i\eta)$ both for negative and positive energy E. Moreover, as a self-consistent check, one can show that $f_m(E)$ becomes the same as that in references [31,32], when the spin-orbit coupling is zero, i.e., for $x_+ \to x_-$. Indeed, in this limit, using the L'Hospital's rule and the Bessel differential equation for I_m, it can be shown that the factor multiplied by $P_m(x_+,x_-)$ in equation (39) is exactly zero, and the remaining terms can be rewritten in the same form as that in references [31,32].

The next step is to replace the modified Bessel functions in equation (39) by their uniform approximation [43,32]. Keeping only the leading terms we obtain

$$\mathrm{Tr}\,\hat{G}_H = \frac{m^*R^2}{h^2 x}\sum_{m=-\infty}^{\infty}\left\{\frac{1}{2}\left[\frac{x_+}{m^2+x_+^2} + \frac{x_-}{m^2+x_-^2}\right] + \frac{1}{x_+ + x_-}\left[1 - \frac{2m^2 + x_+^2 + x_-^2}{2\sqrt{(m^2+x_+^2)(m^2+x_-^2)}}\right]\right\}. \tag{40}$$

Note that the second term bracketed in square brackets is zero when $x_+ \to x_-$, and one finds the perimeter term of the DOS for billiards with zero spin-orbit coupling from the remaining terms. Taking into account the subsequent terms in the uniform approximation provides a systematic way to derive higher order terms for the trace of G_H as in reference [32] for normal circular billiards. However, with non-zero spin-orbit coupling the calculations become more cumbersome.

The summation over m in (40) can be rewritten using the Poisson summation formula [28,45]

$$\sum_{m=-\infty}^{\infty} f_m = \sum_{\mu=-\infty}^{\infty}\int_{-\infty}^{\infty} dm f_m\, e^{i2\pi\mu m}. \tag{41}$$

Then, the Weyl series, i.e., the smooth part of the DOS, following Berry and Howls [32], can be obtained by keeping only the $\mu = 0$-term in (41). Carrying out the limiting process, $\eta \to 0$ in the trace of G_H given by equation (40), and using the integral

$$\int_b^a dz\,\frac{2z^2 - a^2 - b^2}{\sqrt{(z^2-b^2)(a^2-z^2)}} = 2(a+b)\left[E\left(\frac{a-b}{a+b}\right) - K\left(\frac{a-b}{a+b}\right)\right], \tag{42}$$

valid for $0 < b < a$ (E and K are the complete elliptic integrals with the same definitions as in reference [44]) for integration over m, we obtain the contribution to the smooth DOS coming from $\mathrm{Tr}\,\hat{G}_H$. A tedious calculation yields

$$\bar{\varrho}_H(\varepsilon) = -\frac{1}{2\sqrt{\varepsilon+\varepsilon_{\mathrm{so}}}} - \sqrt{\varepsilon_{\mathrm{so}}}\,\delta(\varepsilon+\varepsilon_{\mathrm{so}}) - \frac{1}{\pi}\begin{cases}\frac{1}{\sqrt{\varepsilon+\varepsilon_{\mathrm{so}}}}\left[E\left(\sqrt{\frac{\varepsilon_{\mathrm{so}}}{\varepsilon+\varepsilon_{\mathrm{so}}}}\right) - K\left(\sqrt{\frac{\varepsilon_{\mathrm{so}}}{\varepsilon+\varepsilon_{\mathrm{so}}}}\right)\right], & \varepsilon > 0,\\ \frac{\sqrt{\varepsilon_{\mathrm{so}}}}{\varepsilon+\varepsilon_{\mathrm{so}}}\left[E\left(\sqrt{\frac{\varepsilon+\varepsilon_{\mathrm{so}}}{\varepsilon_{\mathrm{so}}}}\right) - K\left(\sqrt{\frac{\varepsilon+\varepsilon_{\mathrm{so}}}{\varepsilon_{\mathrm{so}}}}\right)\right], & \varepsilon < 0,\end{cases} \tag{43}$$

where the dimensionless energies $\varepsilon = 2m^*ER^2/\hbar^2$ and $\varepsilon_{\mathrm{so}} = 2m^*\Delta_{\mathrm{so}}R^2/\hbar^2 = k_{\mathrm{so}}^2R^2$ have been introduced. The first term is the contribution from the first and second terms of equation (40), and it coincides with the perimeter term derived in equation (18) for arbitrary shapes of Rashba billiards. The Dirac delta term and the terms containing the complete elliptic integrals in (43) come from the term involving brackets in (40).

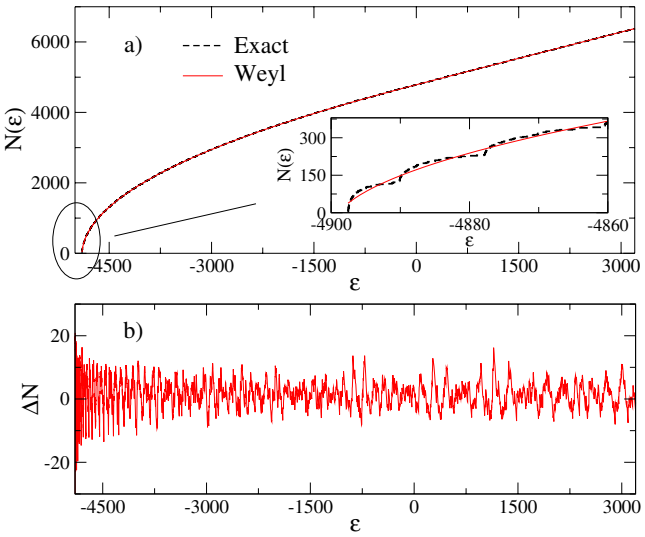

Fig. 1. (Color online) In panel (a) the exact counting function $N(\varepsilon)$ (dashed line) and $\bar{N}(\varepsilon)$ (solid line) are shown for $\sqrt{\varepsilon_{\rm so}} = k_{\rm so}R = 70$. The inset shows the enlarged portion of the main figure close to the bottom of the spectrum. In panel (b) the difference $\Delta N = N(\varepsilon) - \bar{N}(\varepsilon)$ is plotted. In both panels dimensionless energies $\varepsilon = 2m^*ER^2/\hbar^2$ are used.

Finally, including the contribution from $\mathrm{Tr}\,\hat{G}_\infty$, the integration of the DOS over E leads to the smooth counting function $\bar{N}(\varepsilon)$ for Rashba billiards:

$$\bar{N}(\varepsilon) = \begin{cases} \frac{\varepsilon+2\varepsilon_{\rm so}}{2} - \sqrt{\varepsilon+\varepsilon_{\rm so}} + \frac{2}{\pi}\Big[\frac{\varepsilon}{\sqrt{\varepsilon+\varepsilon_{\rm so}}}\,K\left(\sqrt{\frac{\varepsilon_{\rm so}}{\varepsilon+\varepsilon_{\rm so}}}\right) \\ \quad -\sqrt{\varepsilon+\varepsilon_{\rm so}}\,E\left(\sqrt{\frac{\varepsilon_{\rm so}}{\varepsilon+\varepsilon_{\rm so}}}\right)\Big], \ \text{for } \varepsilon > 0, \\ \\ \sqrt{\varepsilon_{\rm so}}\sqrt{\varepsilon+\varepsilon_{\rm so}} - \sqrt{\varepsilon+\varepsilon_{\rm so}} - \frac{2\sqrt{\varepsilon_{\rm so}}}{\pi}\,E\left(\sqrt{\frac{\varepsilon+\varepsilon_{\rm so}}{\varepsilon_{\rm so}}}\right), \\ \quad \text{for } -\varepsilon_{\rm so} < \varepsilon < 0. \end{cases} \tag{44}$$

The first two terms (for both positive and negative energies) are the contribution from $\hat{G}_\infty$. They are the area and perimeter terms in the Weyl series and agree with the results given by (15) and (19), respectively for arbitrary shapes of Rashba billiards. The terms containing the complete elliptic integrals are corrections to the perimeter term in case of circular billiards. We note that in a completely different context, namely for annular ray-splitting billiards, a similar Weyl formula has been calculated [46] involving also elliptic integrals.

We have compared the smooth counting function $\bar{N}(\varepsilon)$ given by equation (44) with the exact counting function $N(\varepsilon)$ calculated from the energy levels obtained from the secular equation (31) for different m. The relevant parameter characterizing a circular Rashba billiard of size R is $k_{\rm so}R$. Typical values for the spin–orbit–induced spin precession length $L_{\rm so} = \pi/k_{\rm so}$ are of the order of a few hundred nanometers [1]. Taking $R = 10$ μm for a typical size of quantum dots, the relevant parameter $k_{\rm so}R$ in Rashba billiards can be as large as 70 (for example, with electric field 10^7 V/m we find for GaAs, GaSb, InAs and InSb that $k_{\rm so}R$ is 3.8, 17.8, 34.5, and 89.2, respectively [47].).

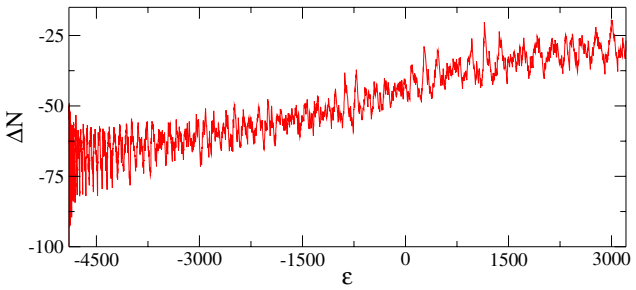

Fig. 2. The difference ΔN between the exact counting function and $\bar{N}(\varepsilon)$ without the terms containing the elliptic integrals in equation (44) is plotted. The energy is scaled as $\varepsilon = 2m^*ER^2/\hbar^2$ and $k_{\rm so}R = 70$.

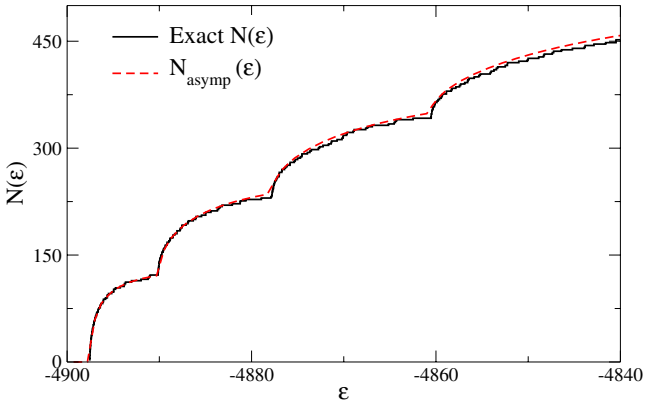

Fig. 3. (Color online) The exact counting function $N(\varepsilon)$ (solid line) and the asymptotic counting function $N_{\rm asymp}(\varepsilon)$ given by equation (48) (dashed line). The energy is scaled as $\varepsilon = 2m^*ER^2/\hbar^2$ and $k_{\rm so}R = 70$.

Figure 1a shows the exact and the smooth counting functions as functions of the dimensionless energy ε. There are 6388 energy levels in the plotted energy range. To see the difference between the two functions, in the inset we plotted them close to the bottom of the energy spectrum. Figure 1b shows the difference $\Delta N = N(\varepsilon) - \bar{N}(\varepsilon)$ as a function of ε. The difference fluctuates around zero, which means we did not miss levels (the mean value of ΔN is a sensitive test for missing levels, see e.g., Ref. [48]). Without correction terms in equation (44) with elliptic integrals, ΔN would increase monotonically on average as shown in Figure 2, and would predict a difference ≈27 in the energy range plotted.

3.3 The counting function for negative energies

In Figure 3, the exact counting function is shown for negative energies near the bottom of the spectrum $-\varepsilon_{\rm so}$. As can be seen the exact $N(\varepsilon)$ shows an additional rounded step structure at certain energies ε_n^*. This feature shows up only for negative energies, although for larger energies this is less pronounced. The step structure results in large deviations ΔN at energies ε_n^* and concomitant large peaks in the DOS.

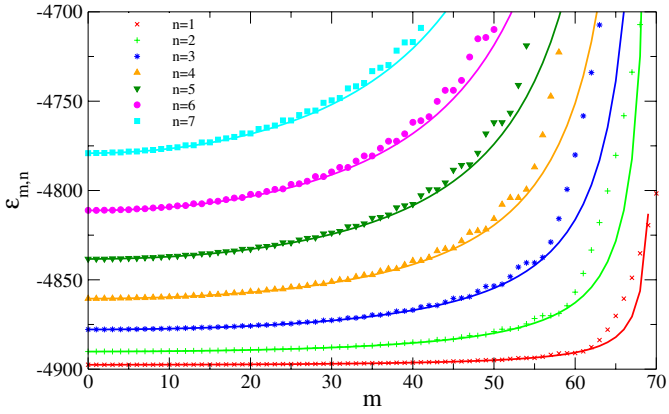

Fig. 4. (Color online) The m dependence of the exact energy levels (in units of $\hbar^2/2m^*R^2$) of circular Rashba billiards (symbols) for a given n ranging from $n = 1$ to $n = 7$. The solid lines are the curves obtained from the approximation of the exact energy levels given by equation (45) as functions of m with the corresponding n. Here $k_{\rm so}R = 70$.

To see the reason for this behavior, it is useful to plot the energy levels as functions of m, as shown in Figure 4. The curves in the figure start almost horizontally at ε_n^*, $n = 1, 2, \ldots$ resulting in large peaks in the DOS at the same energies. Using Debye's asymptotic expression for Bessel functions with large argument [43], we were able to derive the energy dispersion in leading order:

$$\varepsilon_{m,n} = \varepsilon_{\rm so}\left[\frac{\left(\frac{n\pi}{2}\right)^2}{\varepsilon_{\rm so} - m^2} - 1\right] \tag{45}$$

valid only for negative energies. Figure 4 also shows the comparison of the exact energy levels and their approximated m and n dependence given by equation (45). For small m, n the above expression agrees excellently with the numerics (e.g., $\varepsilon_{0,1}$ is accurate up to 7 digits for $\varepsilon_{\rm so} = 70$). The smallest energy level in the spectrum of the circular Rashba billiard is $E_{\rm min} = \hbar^2/(2m^*R^2)\,\varepsilon_{0,1} \cong \hbar^2/(2m^*)\,\pi^2/(4R^2) - \Delta_{\rm so}$.

We now derive an approximated expression for the counting function using

$$N_{\rm asymp}(\varepsilon) = 2\sum_{m=0}^{m_{\rm max}}\sum_{n=1}^{n_{\rm max}}\Theta(\varepsilon - \varepsilon_{m,n}), \tag{46}$$

where $\varepsilon_{m,n}$ are given by equation (45), the factor 2 takes into account the Kramers degeneracy in m, and $m_{\rm max} = [\sqrt{\varepsilon_{\rm so}}\,]$ and $n_{\rm max} = [(2\sqrt{\varepsilon_{\rm so}}/\pi]$ are the largest m and n for which $\varepsilon_{m,n}$ is still negative. Here $[\cdot]$ stands for the integer part. Applying the Poisson summation formula [28,45] in the sum over m in equation (46) and keeping only the non-oscillating term we find

$$\begin{aligned} N_{\rm asymp}(\varepsilon) &= 2\sum_{n=1}^{n_{\rm max}}\int_{-\frac{1}{2}}^{m_{\rm max}+\frac{1}{2}}\Theta(\varepsilon - \varepsilon_{m,n})\,dm \\ &= 2\sum_{n=1}^{n_{\rm max}} m^*(\varepsilon, n), \end{aligned} \tag{47}$$

where $m^*(\varepsilon, n)$ is the solution of $\varepsilon_{m,n} = \varepsilon$ for m at a given ε and n. Thus, from equation (47), after some simple algebra, we obtain the final form of the asymptotic counting function in Debye's approximation:

$$N_{\rm asymp}(\varepsilon) = 2\sqrt{\varepsilon_{\rm so}}\sum_{n=0}^{n_{\rm max}}\sqrt{\frac{\varepsilon - \varepsilon_n^*}{\varepsilon + \varepsilon_{\rm so}}}\,\Theta(\varepsilon - \varepsilon_n^*),\ \text{for } \varepsilon < 0, \tag{48}$$

where $\varepsilon_n^* = \varepsilon_{0,n} = \left(\frac{n\pi}{2}\right)^2 - \varepsilon_{\rm so}$. The result is plotted together with the exact counting function in Figure 3. The agreement is clearly visible near the bottom of the spectrum. However, it is an open question what semi-classical picture can be associated to the content of equation (45). A possible treatment in this direction may be the semi-classical approach of references [40,41].

The density of states is the derivative of the counting function $N(E)$ with respect to E, therefore for circular Rashba billiards in the DOS square root types singularities (van Hove type) appear at energies $E_n^{\rm sing} = \hbar^2/(2m^*R^2)\,\varepsilon_n^*$. This singular behaviour should be detectable by measuring the differential conductance for transport through a Rashba billiard.

3.4 The spin structures of the eigenstates

It is straightforward to obtain corresponding spinor eigenstates and calculate their expectation value for the z component of spin. Similar to the case of Rashba-split eigenstates in rings [13], but in contrast to that of quantum wires [10,11], it turns out to be finite.

The eigenstates of the Rashba billiards satisfying the Dirichlet boundary conditions can be expressed with the linear combination of the regular eigenspinors $|\chi_m^{\pm}\rangle$ given by (26):

$$\begin{aligned} \Psi_{m,n}(r,\varphi) = \frac{1}{\sqrt{\mathcal{N}}}\Bigg\{ & c_+\begin{pmatrix} J_m(k_+r) \\ J_{m+1}(k_+r)\,e^{i\varphi}\end{pmatrix} \\ & + c_-\begin{pmatrix} -J_m(k_-r) \\ J_{m+1}(k_-r)\,e^{i\varphi}\end{pmatrix}\Bigg\} e^{im\varphi}, \end{aligned} \tag{49}$$

where $\mathcal{N}$ is the normalization constant, the coefficients $c_\pm$ satisfy

$$\frac{c_+}{c_-} = \frac{J_m(k_-R)}{J_m(k_+R)} = -\frac{J_{m+1}(k_-R)}{J_{m+1}(k_+R)}, \tag{50}$$

and $k_\pm$ satisfy the secular equation (31) with energy levels $\varepsilon_{m,n}$. Eigenstates given by equation (49) are valid for $\varepsilon_{m,n} > 0$. In the opposite case, one should use the eigenspinor given in (26) for $E < 0$. Regarding the spin structures, it turns out that both cases (the positive and negative energy levels) can be treated at the same level if the definitions for $k_\pm$ in (4) are modified as $k_\pm = k \mp k_{\rm so}$. Therefore, hereafter we use these new definitions for $k_\pm$.

The spin structure of the eigenstates in Rashba billiards can be obtained by calculating the expectation values for spin components:

$$\langle\sigma_i\rangle_{m,n} = \int_0^R\int_0^{2\pi} r dr d\varphi \Psi_{m,n}^+(r,\varphi)\,\sigma_i\,\Psi_{m,n}(r,\varphi), \tag{51}$$

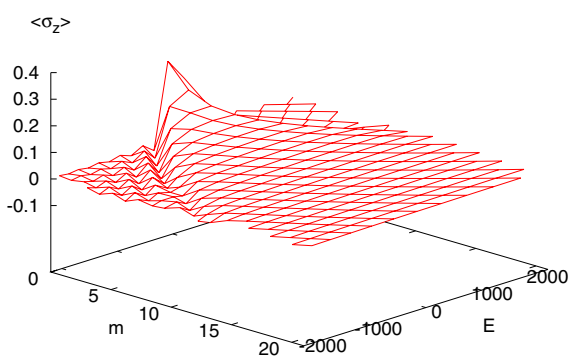

Fig. 5. The expectation values of $\langle\sigma_z\rangle_{m,n}$ as functions of the angular quantum number m and eigenvalues $\varepsilon_{m,n}$ for $k_{\rm so}R = 70$.

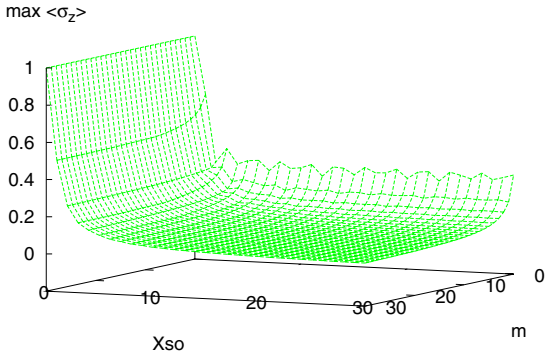

Fig. 6. The maximum of the $\langle\sigma_z\rangle_{m,n}$ as functions of m and $X_{\rm so} = k_{\rm so}R$.

where $i = x, y, z$, and $+$ denotes the transpose and the complex conjugation of a spinor state. The integrand in this equation is the spin density of σ_i. The eigenstates (49) can be written in the form of

$$\Psi_{m,n}(r,\varphi) = \begin{pmatrix} \Psi^{(1)}_{m,n}(r) \\ \Psi^{(2)}_{m,n}(r)e^{i\varphi} \end{pmatrix} e^{im\varphi}, \tag{52}$$

and then it is easy to show that the spin density depends only on r as

$$\Psi^{+}_{m,n}(\mathbf{r})\,\sigma_z\,\Psi_{m,n}(\mathbf{r}) = \left|\Psi^{(1)}_{m,n}(r)\right|^2 - \left|\Psi^{(2)}_{m,n}(r)\right|^2, \tag{53a}$$

$$\Psi^{+}_{m,n}(\mathbf{r})\,\sigma_r\,\Psi_{m,n}(\mathbf{r}) = 2\Psi^{(1)}_{m,n}(r)\Psi^{(2)}_{m,n}(r), \tag{53b}$$

where $\sigma_r = \cos\varphi\sigma_x + \sin\varphi\sigma_y$ is the in-plane radial component of the spin. One can also show that the angular component $\Psi^{+}_{m,n}\,\sigma_\varphi\,\Psi_{m,n}$ of the in-plane spin density is exactly zero, where $\sigma_\varphi = -\sin\varphi\,\sigma_x + \cos\varphi\,\sigma_y$. Therefore, the in-plane spin density at point $\mathbf{r}$ in the billiard is along the radial direction $\mathbf{r}$ [19]. This implies that the expectation values for in-plane spin is zero, i.e., $\langle\sigma_x\rangle_{m,n} = \langle\sigma_y\rangle_{m,n} = 0$.

Performing the integration (that can be carried out analytically) in equation (51) for $\langle\sigma_z\rangle_{m,n}$ we find

$$\langle\sigma_z\rangle_{m,n} = -\frac{\varepsilon_{m,n} + \varepsilon_{\rm so}}{\sqrt{\varepsilon_{\rm so}}} \times \frac{1}{\left[\frac{J_m(k_-R)}{J_{m+1}(k_-R)} + \frac{J_{m+1}(k_-R)}{J_m(k_-R)}\right]\varepsilon_{m,n} + (2m+1)\sqrt{\varepsilon_{\rm so}}}. \tag{54}$$

This is an exact analytic result for the expectation values of the z component of the spin for circular Rashba billiards.

Figure 5 shows the expectation values of $\langle\sigma_z\rangle_{m,n}$ calculated numerically from (54) for different angular quantum number m and eigenvalues $\varepsilon_{m,n}$ with a given Rashba coupling strength α. One can see from the figure that $\langle\sigma_z\rangle_{m,n}$ has a peak at $m = 0$ and for eigenvalue $\varepsilon_{m,n}$ close to zero. We have studied how this peak value changes for different Rashba coupling strength α. For each $k_{\rm so}R$ and m the maximum of $\langle\sigma_z\rangle_{m,n}$ over the eigenvalues $\varepsilon_{m,n}$ is plotted in Figure 6. It is clear from the figure that the expectation values of $\langle\sigma_z\rangle_{m,n}$ is robust for different Rashba coupling strength α.

For Rashba billiards, in weak magnetic field the energy levels of the Kramers doublets will be splitted by the Zeeman effect. Using the first order perturbation valid for weak field limit, i.e., when the cyclotron radius is much larger than the size of the Rashba billiard, the values of the Zeeman splitting is proportional to the expectation values of $\langle\sigma_z\rangle_{m,n}$. Thus, we believe that the significant magnitude of the spin z component found from our numerical results can be detectable experimentally.

4 Conclusions

Before concluding in this section we briefly summarize our results not discussed in this paper on the statistics of energy levels, and highlight some open theoretical problems in connection with Rashba billiards.

The Schrödinger equation (including boundary conditions) for circular Rashba billiards is separable in polar coordinates, thus integrable. Hence, the statistics of energy levels should be Poissonian (see e.g. Ref. [34]). Indeed, we have found that the nearest-neighbor level-spacing distribution $P(s)$ is Poissonian (not shown here). For other shapes of Rashba billiards, spin-orbit coupling may destroy integrability, in which case Random Matrix Theory (RMT) predicts that the level statistics should be governed by the symplectic ensemble [34,49]. Note, however, that some intermediate distribution (not described by RMT) was found [23] for a rectangularly shaped billiard with Dirichlet boundary conditions in the limit of small

$k_{\rm so}$, reflecting the fact that a rectangular billiard is integrable in the absence of SO coupling but non-integrable when SO is finite.

We now list a few interesting open theoretical problems. The Weyl formula is essential to develop a periodic orbit theory for Rashba billiards. (For normal billiards, see Brack and Bhaduri's book in Ref. [27,28], and a theory in case of harmonically confined Rashba systems is given in Ref. [41].) To get better insight into the dynamics of Rashba billiard systems, one can develop a semiclassical analysis used by Littlejohn and Flynn [40]. The Green's function method presented in this work would be a suitable starting point to calculate observables such as the magnetization [50] or persistent currents [13] in Rashba billiards.

Our calculation presented in this work remains valid when only the Dresselhaus coupling is non-zero in the Hamiltonian since with a unitary transformation the Hamiltonian of the Dresselhaus billiard can be transformed to that of the Rashba billiard. However, the semiclassical analysis still remain a challenge for further research when both the Dresselhaus and the Rashba coupling constants are non-zero (except the case when they are equal [51]).

We have so far left undiscussed any issues related to disorder effects. While these warrant a separate thorough study, a qualitative consideration of their impact is possible already within the framework of this article. For our purposes, two types of disorder are relevant: (i) potential disorder whose effect in the presence of Rashba spin splitting was considered, e.g., in reference [52], and (ii) randomness in the structural inversion asymmetry that determines the Rashba coefficient [53]. To be able to safely neglect disorder of type (i), the billiard's size has to be smaller than the electronic mean free path. Also, type-(ii) disorder will be irrelevant if the fluctuations in the Rashba coefficient α are much smaller than its average value. The thus defined clean limit is certainly within reach of current nanofabrication technology [12] where typical values of the mean free path routinely exceed several microns and Rashba spin splitting is large. However, most of our results presented in this study remain valid for sufficiently weak disorder such that its bandwidth $\Gamma_{\rm r}$ is smaller than the spin-orbit energy scale $\Delta_{\rm so}$. Furthermore, the singularities found in the DOS at (small) negative energies will be washed out only for $\Gamma_{\rm r} > \sqrt{\varepsilon_{\rm so}}\,\hbar^2/(mR^2)$.

In conclusion, we have presented a study of electron billiards with spin-dependent dynamics due to Rashba spin splitting. Semi-classical results for the spectrum agree well with exact quantum calculations for circular billiards, and we find interesting properties of negative-energy states, including a finite spin projection in the out-of-plane direction.

This work is supported in part by E.C. Contract No. MRTN-CT-2003-504574, and the Hungarian Science Foundation OTKA T034832, T046129 and T038202. U.Z. gratefully acknowledges funding from the Marsden Fund of the Royal Society of New Zealand.

References

1. *Semiconductor Spintronics and Quantum Computation*, edited by D.D. Awschalom, D. Loss, N. Samarth (Springer, Berlin, 2002)
2. S.A. Wolf, D.D. Awschalom, R.A. Buhrman, J.M. Daughton, S. von Molnár, M.L. Roukes, A.Y. Chtchelkanova, D.M. Treger, Science **294**, 1488 (2001)
3. G. Lommer, F. Malcher, U. Rössler, Phys. Rev. Lett. **60**, 728 (1988)
4. E.I. Rashba, Fiz. Tverd. Tela (Leningrad) **2**, 1224 (1960); [Sov. Phys. Solid State **2**, 1109 (1960)]
5. J. Nitta, T. Akazaki, H. Takayanagi, T. Enoki, Phys. Rev. Lett. **78**, 1335 (1997)
6. T. Schäpers, G. Engels, J. Lange, Th. Klocke, M. Hollfelder, H. Lüth, J. Appl. Phys. **83**, 4324 (1998)
7. Y. Sato, T. Kita, S. Gozu, S. Yamada, J. Appl. Phys. **89**, 8017 (2001)
8. S. Datta, B. Das, Appl. Phys. Lett. **56**, 665 (1990)
9. F. Mireles, G. Kirczenow, Phys. Rev. B **64**, 024426 (2001)
10. W. Häusler, Phys. Rev. B **63**, 121310(R) (2001)
11. M. Governale, U. Zülicke, Phys. Rev. B **66**, 073311 (2002)
12. T. Schäpers, J. Knobbe, V.A. Guzenko, Phys. Rev. B **69**, 235323 (2004)
13. J. Splettstoesser, M. Governale, U. Zülicke, Phys. Rev. B **68**, 165341 (2003)
14. P. Földi, B. Molnár, M.G. Benedict, F.M. Peeters, Phys. Rev. B **71**, 033309 (2005)
15. O. Voskoboynikov, C.P. Lee, O. Tretyak, Phys. Rev. B **63**, 165306 (2001)
16. M. Governale, Phys. Rev. Lett. **89**, 206802 (2002)
17. M. Valín-Rodríguez, A. Puente, L. Serra, Phys. Rev. B **69**, 085306 (2004)
18. E.N. Bulgakov, A.F. Sadreev, Phys. Rev. B **66**, 075331 (2002)
19. M. Valín-Rodríguez, A. Puente, L. Serra, Phys. Rev. B **69**, 153308(R) (2004)
20. C.F. Destefani, S.E. Ulloa, G.E. Marques, Phys. Rev. B **69**, 125302(R) (2004)
21. O. Zaitsev, D. Frustaglia, K. Richter, Phys. Rev. Lett. **94**, 026809 (2005)
22. E.N. Bulgakov, A.F. Sadreev, JETP Letters **78**, 443 (2003); E.N. Bulgakov, A.F. Sadreev, Phys. Rev. E **70**, 056211 (2004); A.I. Saichev, H. Ishio, A.F. Sadreev, K.-F. Berggren, J. Phys. A **35**, L87 (2002)
23. K.-F. Berggren, T. Ouchterlony, Found. Phys. **31**, 233 (2001)
24. I.L. Aleiner, V.I. Fal'ko, Phys. Rev. Lett. **87**, 256801 (2001); J.-H. Cremers, P.W. Brouwer, V.I. Fal'ko, Phys. Rev. B **68**, 125329 (2003)
25. Yu.A. Bychkov, E.I. Rashba, J. Phys. C **17**, 6039 (1884)
26. H. Weyl, Göttinger Nachrichten **110**, 114 (1911)
27. H.T. Baltes, E.R. Hilf, *Spectra of Finite Systems* (Bibliographisches Institut Wissenschaftsverlag, Mannheim, 1976)
28. M. Brack, R.K. Bhaduri, *Semiclassical Physics* (Addison-Wesley, Reading, 1997
29. M. Kac, Am. Math. Monthly **73**, 1 (1966)
30. R. Balian, C. Bloch, Ann. Phys. (N.Y.) **60**, 401 (1970)
31. K. Stewartson, R.T. Waechter, Proc. Cambridge Philos. Soc. **69**, 581 (1971)
32. M. Berry, C.J. Howls, Proc. R. Soc. Lond. A **447**, 527 (1994)

33. M. Sieber, H. Primack, U. Smilansky, I. Ussishkin, H. Schanz, J. Phys. A **28**, 5041 (1995)
34. *Chaos and Quantum Physics*, edited by M.-J. Giannoni, A. Voros, J. Zinn-Justin (Elsevier Science Publishers B.V., Amsterdam, The Netherlands, 1991)
35. M.V. Berry, R.J. Mondragon, Proc. R. Soc. Lond. A **412**, 53 (1987)
36. E.N. Bulgakov, A.F. Sadreev, JETP Letters **73**, 505 (2001)
37. E. Tsitsishvili, G.S. Lozano, A.O. Gogolin, Phys. Rev. B **70**, 115316 (2004)
38. C.-H. Chang, A.G. Mal'shukov, K.A. Chao, Phys. Rev. B **70**, 245309 (2004)
39. J. Cserti, A. Csordás, U. Zülicke, Phys. Rev. B **70**, 233307 (2004)
40. R.G. Littlejohn, W.G. Flynn, Phys. Rev. A **45**, 7697 (1992)
41. M. Pletyukhov, Ch. Amann, M. Mehta, M. Brack, Phys. Rev. Lett. **89**, 116601 (2002); Ch. Amann, M. Brack, J. Phys. A **35**, 6009 (2002)
42. J.D. Walls, J. Huang, R.M. Westervelt, E.J. Heller, e-print `arXiv:cond-mat/0507528`
43. M. Abramowitz, I.A. Stegun, *Handbook of Mathematical Functions* (Dover, New-York, 1972)
44. I.S. Gradshteyn, I.M. Ryzhik, *Table of Integrals, Series, and Products*, 5th edn. (Academic Press, San Diego, 1994)
45. M. Berry in reference [34], p. 251
46. Y. Décanini, A. Folacci, Phys. Rev. E **68**, 046204 (2003)
47. R. de Sousa, S. Das Sarma, Phys. Rev. B **68**, 155330 (2003)
48. C. Schmit in reference [34], p. 331; A. Csordás, R. Graham, P. Szépfalusy, Phys. Rev. A **44**, 1491 (1991)
49. C.W.J. Beenakker, Rev. Mod. Phys. **69**, 731 (1997)
50. E.A. de Andrada e Silva, G.C. La Rocca, F. Bassani, Phys. Rev. B **50**, 8523 (1994)
51. J. Schliemann, J. Carlos Egues, D. Loss, Phys. Rev. Lett. **90**, 146801 (2003)
52. V.N. Gridnev, JETP Lett. **74**, 380 (2001)
53. E.Ya. Sherman, Appl. Phys. Lett. **82**, 209 (2003); L.E. Golub, E.L. Ivchenko, Phys. Rev. B **69**, 115333 (2004); M.M. Glazov, E.Ya. Sherman, Phys. Rev. B **71**, 241312(R) (2005); E.Ya. Sherman, D.J. Lockwood, Phys. Rev. B **72**, 125314 (2005)